

Superexchange-Coupled Electron-Spin Pairs in Iron Tetraphenylporphyrin Chloride at Low Temperatures*

G. L. Neiheisel, J. L. Imes, and W. P. Pratt, Jr.

Department of Physics, Michigan State University, East Lansing, Michigan 48824

(Received 19 May 1975)

Magnetic susceptibility, heat capacity, and EPR studies reported here show that close to 50% of the high-spin Fe^{3+} ions in this compound form isolated spin pairs each of which shows a highly anisotropic superexchange coupling. Direct EPR transitions between the superexchange-split energy levels have been observed.

The metalloporphyrins are a class of organometallic complexes which have been extensively studied because of their inclusion in certain biological molecules such as myoglobin, hemoglobin, chlorophyll, etc.¹ The paramagnetic forms of the metallo-tetraphenylporphyrins typically can have nearest-neighbor distances between paramagnetic sites in excess of 8 Å.² The magnetic interaction between these sites is expected to be primarily the classical magnetic dipole-dipole coupling with resulting millikelvin-range magnetic-ordering temperatures. The ultralow-temperature behavior of copper tetraphenylporphine does satisfy these expectations.³ However, iron tetraphenylporphyrin chloride (FeTPPCl) exhibits magnetic correlation effects in its susceptibility and heat capacity at temperatures near 1 K. In this paper we shall show that this compound possesses the following interesting properties:

(a) Close to 50% of the high-spin Fe^{3+} ions form electron-spin pairs, each coupled via a superexchange mechanism—a significant addition to the small list of undiluted compounds in which isolated spin-pairs occur.⁴

(b) The superexchange coupling is highly anisotropic, which is unusual for *S*-state ions, and is large compared to the classical dipole-dipole coupling between the Fe^{3+} spins.

(c) The energy splittings due to this superexchange coupling are small in comparison to the energy splittings of each Fe^{3+} ion associated with the crystal-electric-field parameter D_c [see Eq. (1)].

(d) These superexchange energy splittings in zero magnetic field fall within the microwave range of frequencies, 8 to 28 GHz. We have been able to observe direct transitions between these energy levels with an EPR spectrometer, including forbidden magnetic dipole transitions.

Details of the ^3He - ^4He dilution refrigerator and the apparatus used in the susceptibility and the heat-capacity measurements will appear elsewhere.⁵ Polycrystalline samples of FeTPPCl were obtained commercially.⁶ A 0.1-mg single crystal was grown in a 1:2 mixture of dichloromethane and hexane, and its expected crystal structure was confirmed by x-ray analysis. The susceptibilities both parallel and perpendicular to the *c* axis of this crystal were measured in magnetic fields of 2.5 and 0.25 mT, respectively. A superconducting-quantum-interference-device (SQUID) magnetometer of standard design was employed.⁷ For the heat-capacity experiment, a 1.58-g polycrystalline sample was used. In order to improve the thermal contact between the grains, we heated this sample and added 0.07 g of liquid Apiezon-*N* grease to it. The internal thermal equilibrium time was as long as several hours at temperatures near 100 mK.

The inset of Fig. 1 depicts the planar porphyrin molecule with the Fe^{3+} ion, the four phenyl ligands, and the chloride ligand attached. Two body-centered tetragonal unit cells are also shown in Fig. 1. X-ray studies indicate an orientational disorder for these molecules.⁸ The chloride ions can, with apparently equal probability, be situated on either side of the porphyrin plane. For 50% of the molecules we assume that the indicated 1 Å separation of the chloride ions should allow some orbital overlap between them and thereby provide a superexchange path between the associated Fe^{3+} ions.

As shown in Fig. 2 the two magnetic susceptibilities deviate from a simple Curie law below 1 K, and the heat capacity passes through a maximum around 0.2 K. In order to interpret these results we choose the following spin Hamiltonian to represent the square-pyramidal coordination of the *i*th Fe^{3+} ion, omitting spin-spin interac-

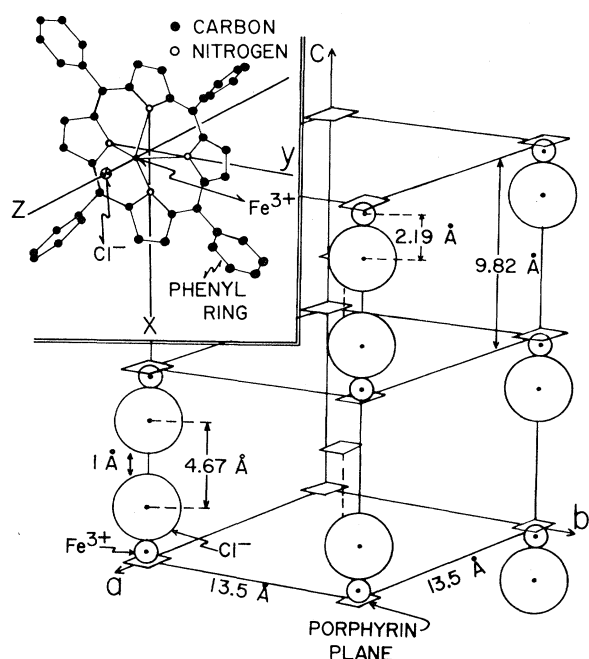


FIG. 1. Diagram of an FeTPPCl molecule and two body-centered tetragonal unit cells. The unit cells are drawn to scale only along the c axis. The spheres representing the ionic radii are drawn to scale.

tions:

$$\mathcal{H}_i = g\mu_B \vec{S}_i \cdot \vec{H} + D_c [S_{iz}^2 - \frac{1}{3}S(S+1)], \quad (1)$$

where z is along the c axis, $S_i = \frac{5}{2}$, $g = 2.00$, and $D_c/k_B \approx 13$ K. This choice of parameters is based on far-infrared-absorption⁹ and EPR studies of other iron-chloride porphyrins¹⁰ and on a comparison of the magnetic susceptibilities of these other porphyrins with FeTPPCl.¹¹ Our EPR studies of FeTPPCl are in agreement with this choice of the g factor.

We choose an anisotropic Heisenberg Hamiltonian to represent the superexchange coupling, and we shall treat as negligible the classical magnetic dipole-dipole coupling between all the Fe^{3+} spins. Our total spin Hamiltonian for a given spin pair is

$$\mathcal{H} = \mathcal{H}_i + \mathcal{H}_j + J_{\parallel} S_{iz} S_{jz} + J_{\perp} (S_{ix} S_{jx} + S_{iy} S_{jy}). \quad (2)$$

A straightforward calculation produces the solid curves in Fig. 2 which are in good agreement with the experimental data. The parameters for the curves are $J_{\parallel}/k_B = -0.40 \pm 0.03$ K, $J_{\perp}/k_B = +0.152 \pm 0.003$ K, and $\alpha = 0.51 \pm 0.01$, where α is the fraction of Fe^{3+} spins in FeTPPCl which form pairs. This value of α is in good agreement with our expectation of $\alpha = 0.50$.

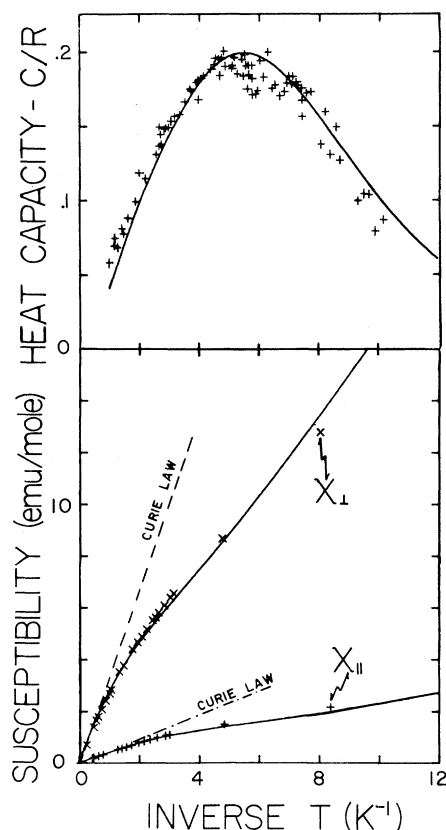


FIG. 2. Temperature dependence of the molar susceptibility and heat capacity of FeTPPCl. The susceptibilities χ_{\parallel} and χ_{\perp} were measured, respectively, with the magnetic field at 10° and 90° with respect to the c axis of the single crystal. C is the heat capacity per mole of FeTPPCl, and R is the molar gas constant. The solid curves represent theoretical calculations discussed in the text.

These values of J_{\parallel} and J_{\perp} were used to calculate the four lowest energy levels shown in Fig. 3. These exchange splittings are small compared to their separation from the next sets of levels approximately $2D_c$ higher in energy. For convenience the energy levels are given singlet-triplet labels as if $S_i = S_j = \frac{1}{2}$. The wide arrows in Fig. 3 represent EPR transitions observed with an 8-mg powdered sample. The length of each arrow is drawn to scale and is plotted for the field at which each rather broad resonance reached a maximum. The thin arrow represents a transition seen for a 0.05-mg single crystal with its c axis at approximately 10° to the external field. The shaded region symbolizes those singlet-triplet transitions where poorly defined maxima were observed at low fields in the range 9.0 to 9.5 GHz. Clearly, these observed transitions give a rather strong

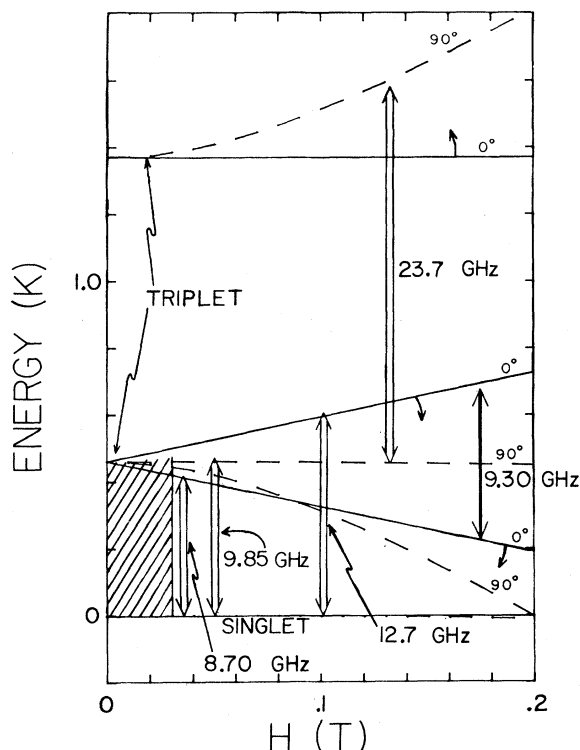


FIG. 3. Energy-level diagram for superexchange-coupled pairs at 0° and 90° orientations of the c axis with respect to an external magnetic field (in teslas). The short curved arrows indicate the direction that these energy levels shift as the field is rotated from 0° toward 90° . The remaining symbols are explained in the text.

first-order confirmation of the simple exchange Hamiltonian. An EPR study of a several-milligram single crystal would significantly improve the precision of the superexchange parameters, particularly J_{\parallel} , and probably would uncover the limitations of the assumed superexchange Hamiltonian.

For this exchange Hamiltonian the singlet-triplet transitions are forbidden magnetic dipole transitions. These forbidden transitions can be clearly distinguished from the allowed transitions when the external magnetic field is placed parallel to the microwave magnetic field. Possibly the exchange Hamiltonian contains an antisymmetric term of the Dzialoshinski-Moriya type, $\mathcal{H}_{ij} = \vec{C} \cdot (\vec{S}_i \times \vec{S}_j)$, which would allow magnetic dipole transitions between the singlet-triplet states.^{12,13}

The superexchange coupling is highly anisotropic and can be alternatively expressed in an isotropic-plus-pseudodipolar form:

$$\mathcal{H}_{ij} = +J\vec{S}_i \cdot \vec{S}_j + D_E(3S_{iz}S_{jz} - \vec{S}_i \cdot \vec{S}_j), \quad (3)$$

where $J/k_B = -0.03 \pm 0.01$ K and $D_E/k_B = -0.18 \pm 0.01$ K. The 9.05-Å distance between the two Fe^{3+} ions in a spin-pair gives a classical dipole coupling parameter of $D_d/k_B = -0.003$ K which is negligible in comparison to the pseudodipolar exchange parameter D_E . Thus the superexchange coupling seems to be primarily pseudodipolar in nature. As originally pointed out by Van Vleck,¹⁴ pseudodipolar exchange can arise from spin-orbit effects.⁴ Since spin-orbit coupling to a rather low-lying excited state of the Fe^{3+} ion is responsible for the unusually large crystal field parameter D_c ,¹⁵ it is suggested that such spin-orbit coupling may be the origin of this pseudodipolar superexchange.

In conclusion, we wish to re-emphasize the point that further EPR studies of FeTPPCl should provide a very well-characterized superexchange coupling. Further, we wish to point out that there are iodide and bromide forms of the high-spin Fe^{3+} tetraphenylporphyrins. Although their crystal structures are not known, certainly the possibility of spin pairing exists. The superexchange coupling for these compounds would probably be different because of the larger ionic radii of the halogen ligands.

We wish to thank Dr. J. A. Cowen for providing the EPR spectrometer and Mr. P. R. Newman for assisting us in its operation. We also acknowledge very useful conversations with Dr. R. D. Spence, Dr. T. A. Kaplan, Dr. S. D. Mahanti, and Dr. M. Barma.

*Work supported by the National Science Foundation and Research Corporation.

¹J. L. Hoard, *Science* **174**, 1295 (1971).

²E. B. Fleischer, *Accounts Chem. Res.* **3**, 105 (1970).

³J. L. Imes, G. L. Neiheisel, and W. P. Pratt, Jr., *Phys. Lett.* **49A**, 351 (1974).

⁴J. Owen and E. A. Harris, in *Electron Paramagnetic Resonance*, edited by S. Geschwind (Plenum, New York, 1972), p. 427, and references therein.

⁵J. L. Imes, G. L. Neiheisel, and W. P. Pratt, Jr., two papers to be published.

⁶Strem Chemicals, Inc., 150 Andover St., Danvers, Mass. 01923.

⁷R. P. Giffard, R. A. Webb, and J. C. Wheatley, *J. Low Temp. Phys.* **6**, 533 (1972).

⁸J. L. Hoard, G. H. Cohen, and M. D. Glick, *J. Amer. Chem. Soc.* **89**, 1992 (1967).

⁹G. C. Brackett, P. L. Richards, and W. S. Caughey, *J. Chem. Phys.* **54**, 4383 (1971).

¹⁰C. P. Scholes, *J. Chem. Phys.* **52**, 4890 (1970).

¹¹C. Maricondi, W. Swift, and D. K. Straub, *J. Amer. Chem. Soc.* **91**, 5205 (1969).

¹²I. Dzialoshinsky, *J. Phys. Chem. Solids* **4**, 241

(1958).

¹³T. Moriya, in *Magnetism*, edited by G. T. Rado and H. Suhl (Academic, New York, 1963), p. 85.¹⁴J. H. Van Vleck, *Phys. Rev.* **52**, 1178 (1937).¹⁵P. S. Han, T. P. Das, and M. F. Rettig, *J. Chem. Phys.* **56**, 3861 (1972), and references therein.

High-Pressure Effects on the Superconducting Transition Temperature of Aluminum

D. U. Gubser and A. W. Webb
Naval Research Laboratory, Washington, D. C. 20375
 (Received 14 April 1975)

The superconducting transition temperature T_c of aluminum has been measured as a function of pressure to 62 kbar, at which point T_c was reduced to 0.075 K from its zero pressure value of 1.18 K. These data cover ranges of temperature and pressure which allow differentiation between theoretical and empirical predictions. The data clearly obey the empirical relation of Smith and Chu and suggest a new volume dependence for the electron-phonon interaction.

Several theoretical models¹⁻¹⁰ have been proposed to explain the effects of hydrostatic pressure P on the superconducting transition temperature T_c of nontransition metal superconductors. Calculations of $T_c(P)$ have been reasonably successful in explaining the reduction of T_c at low pressures (0 to 20 kbar); however, the effects of higher pressures remain uncertain. Smith and Chu¹¹ proposed an empirical relation which described the pressure effects of T_c up to 20 kbar and suggested its validity at even higher pressures. The relation is

$$\Delta T_c / T_0 = \alpha \Delta V / V_0, \quad (1)$$

where T_0 is the zero-pressure transition temperature, V_0 is the zero-pressure atomic volume, ΔV is the change in volume induced by hydrostatic pressure, and α is a material-dependent constant. None of the theoretical models describing the volume (pressure) effects on T_c predict a volume dependence of this form at pressures over 20 kbar.

In this Letter we report the results of our study on the pressure dependence of T_c in aluminum. The data cover ranges of temperature and pressure which for the first time allow differentiation between the various theoretical and empirical predictions. The transition temperature of Al was reduced to less than $\frac{1}{10}$ of its zero-pressure value ($T_0 = 1.18$ K) at a pressure of 62 kbar which represents the largest pressure-induced percentage reduction in T_c ever reported.

Details of the pressure cryostat for achieving the required temperatures and pressures are described elsewhere¹² but are briefly reviewed here

since it has some unique features. Figure 1 shows a cross-section drawing of the pressure cell used for achieving $P \leq 100$ kbar and $T \geq 0.025$ K. A 0.1-mm-diam Al sample is contained in a hardened BeCu gasket and positioned between two diamond anvils each having 0.5-mm faces. Pressure produced between these anvils is controlled hydraulically by externally regulating the ⁴He fluid pressure in a large bellows which drives a piston holding the top diamond. This feature permits acquisition of data over the entire pressure span in one run. Sample pressures are proportional to the externally measured ⁴He pressures. The system was calibrated against published Al data up to 20 kbar.¹³

The BeCu pressure cell is an integral part of a dilution refrigerator. The top plate of the cell contains a small annular cavity which is the mix-

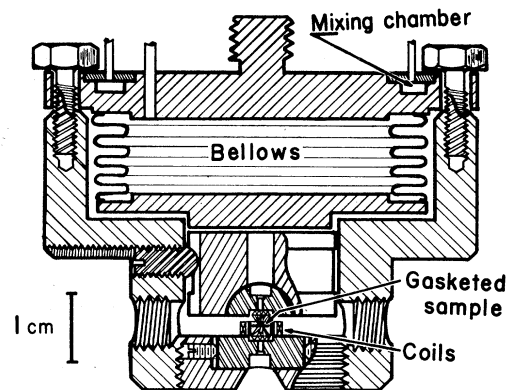


FIG. 1. Cross section of the variable-pressure, low-temperature, diamond-anvil cell.